

Robust Stability Example #1

A. Overview

These notes are taken from Example 7.6 in *Multivariable Feedback Control: Analysis and Design*, S. Skogestad and I. Postlethwaite, John Wiley & Sons, Chichester, UK, 1996, pp. 271-272. That example is expanded with some additional graphs and commentary and a slightly different transfer function approximating the relative uncertainty magnitude. A brief derivation of the condition for robust stability of a family of systems defined by unstructured multiplicative perturbations to a nominal system model is also provided here. The notation used in these notes follows the text's example.

B. Condition for Robust Stability

It is assumed that there is a particular single-input, single-output (SISO) system described in transfer function form that the user desires to control. This is known as the nominal system, and the model describing that system is the transfer function $G(s)$. However, for a variety of reasons closed-loop stability must be provided for a number of other system models as well. These other models might represent various failure modes of the nominal system, uncertainties in the model due to lack of knowledge, or perturbations to the nominal model due to manufacturing tolerances. Other possibilities also exist. In any case, closed-loop stability must be provided for each of the possible system models. This is the robust stability (**RS**) problem.

This family of system models (plants) that must be stabilized is denoted by $G_P(s)$. Depending on the physical nature of the perturbations, various mathematical models for the family of systems can be used. In these notes, and in the text's example, an unstructured multiplicative perturbation to the nominal plant will be used. Thus, the family of plants can be represented by

$$G_P(s) = G(s) [1 + w_I(s)\Delta_I(s)], \quad \|\Delta_I(s)\|_\infty \leq 1 \quad (1)$$

where $w_I(s)$ is a frequency-selective weighting factor, and the stable norm-bounded function $\Delta_I = \rho e^{j\theta}$ is allowed to take on any phase shift. Assuming that the compensator's transfer function is $K(s)$, the loop gain is $L(s) = G(s)K(s)$ for the nominal system, and for the family of plants the loop gain is $L_P(s) = G_P(s)K(s)$. Therefore, in terms of the perturbation model in (1), the family of loop gains is

$$L_P(s) = L(s) [1 + w_I(s)\Delta_I(s)] = L(s) + w_I(s)L(s)\Delta_I(s), \quad \|\Delta_I(s)\|_\infty \leq 1 \quad (2)$$

The term $w_I(s)L(s)\Delta_I(s)$ is the total perturbation to the nominal system $L(s)$, and $w_I(s)\Delta_I(s)$ is the relative perturbation with this multiplicative uncertainty model.

The development of the condition for robust stability will be done in the frequency domain, which can be easily visualized through the use of polar plots in a complex plane. Whenever $|\Delta_I(j\omega)| = \rho = 1$, the total perturbation $w_I(j\omega)L(j\omega)\Delta_I(j\omega)$ at that frequency is at its maximum magnitude, $|w_I(j\omega)L(j\omega)|$. Under this condition, a point in the complex plane representing a particular perturbed system $L'(j\omega) \in L_P(j\omega)$ is as far away as possible from the point representing the nominal system $L(j\omega)$ as any system in the family. The corresponding $L'(s)$ will be referred to as an extreme model. The orientation of this extreme model depends on $\angle\Delta_I(j\omega) = \theta$.

The relationships between the nominal system, a maximum perturbation, and the corresponding extreme model are shown in Figs. 1 and 2. Vectors representing $L(j\omega)$ and a maximum $w_I(j\omega)L(j\omega)$ at frequency ω_i are shown in Fig. 1. The circle at $L(j\omega_i)$ indicates one point on the system's polar plot, which might be used to evaluate the Nyquist stability criterion. The circle at $w_I(j\omega_i)L(j\omega_i)$ corresponds to $\rho = 1$ and some value for θ . In Fig. 2 are shown the vectors for the nominal system at the same value of ω and the extreme system model $L'(j\omega_i) = L(j\omega_i) + w_I(j\omega_i)L(j\omega_i)$ corresponding to the maximum perturbation in Fig. 1. The vector for the perturbation $w_I(j\omega_i)L(j\omega_i)$ is just displaced from the origin to the point $L(j\omega_i)$ in order to create the extreme perturbed system.

As $|\Delta_I(j\omega)|$ takes on all values $\rho \leq 1$ and $\angle\Delta_I(j\omega)$ takes on all values $-\pi \leq \theta < \pi$, the complete family of systems to be stabilized is formed. A closed disc in the complex plane is generated, centered at the nominal system $L(j\omega)$. This is illustrated in Fig. 3 at $\omega = \omega_i$. Each point on and inside the circle of radius $|w_I(j\omega_i)L(j\omega_i)|$ centered at $L(j\omega_i)$ represents the complex value of a particular element of $L_P(j\omega_i)$. The complex values of all the extreme system models will be on this circle, which will be referred to as the circle of uncertainty. Points inside the circle represent perturbed systems generated for values of $\rho < 1$.

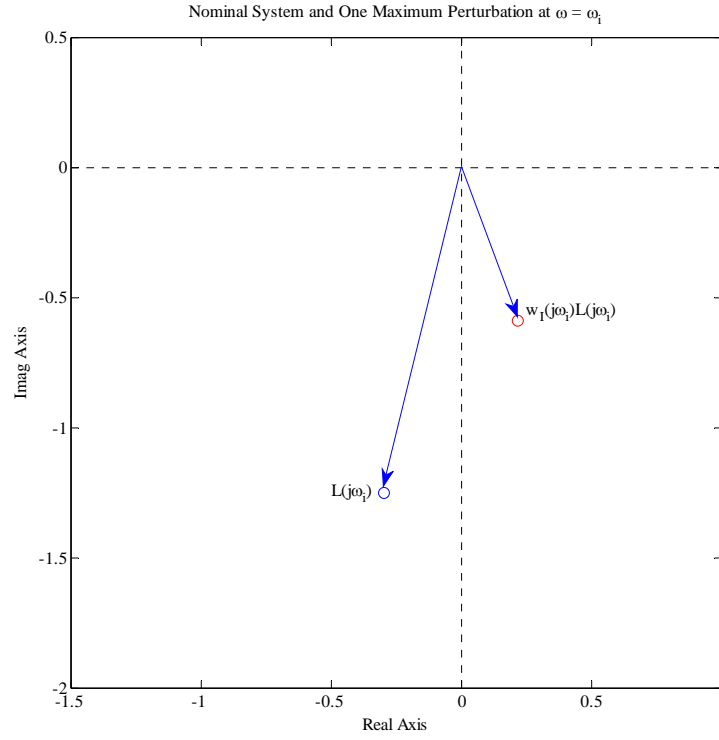


Fig. 1. A nominal loop gain $L(j\omega)$ and an extreme perturbation to that system, evaluated at $\omega = \omega_i$.

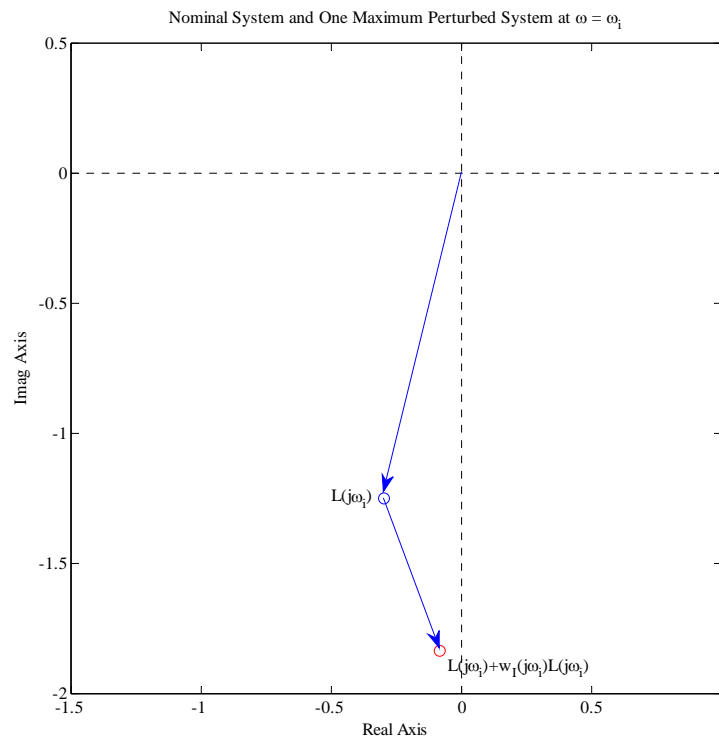


Fig. 2. A nominal loop gain $L(j\omega)$ and an extreme perturbed system $L(j\omega) + w_I(j\omega)L(j\omega)$, evaluated at $\omega = \omega_i$.

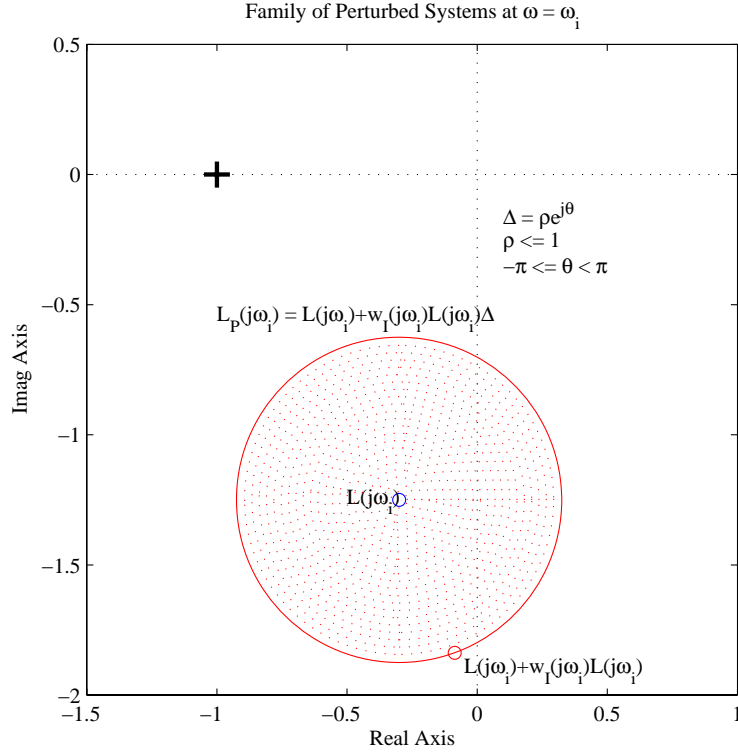


Fig. 3. Family of perturbed systems of $L(s)$, evaluated at $\omega = \omega_i$.

The requirement for robust stability for this family of systems can now be stated. The condition is illustrated graphically in Fig. 4, which shows the same circle of uncertainty as in Fig. 3. The distance from the point $-1 + j0$ to the point $L(j\omega_i)$ is $|1 + L(j\omega_i)|$. In order for the nominal system to be closed-loop stable, its polar plot—assuming that $L(s)$ has no poles in the open right-half plane—must not encircle the -1 point. The same statement is true for each member of the family $L_P(s)$; none of the corresponding polar plots may encircle the -1 point. Therefore, in order for the family of systems $L_P(s)$ to be robustly stable, the circle of uncertainty, with radius $|w_I(j\omega) L(j\omega)|$, must not encircle or intersect the -1 point at any frequency. It can be seen from Fig. 4 that the condition of robust stability imposes the following constraints.

$$|w_I(j\omega) L(j\omega)| < |1 + L(j\omega)|, \forall \omega \quad (3)$$

$$\frac{|w_I(j\omega) L(j\omega)|}{|1 + L(j\omega)|} = |w_I(j\omega) T(j\omega)| < 1, \forall \omega \quad (4)$$

$$|T(j\omega)| < \frac{1}{|w_I(j\omega)|}, \forall \omega \quad (5)$$

where $T(j\omega)$ is the frequency response of the complementary sensitivity function of the nominal system. The condition of robust stability for a family of systems modeled by unstructured multiplicative perturbations to a nominal system normally will be expressed by $|w_I(j\omega) T(j\omega)| < 1$ or $|T(j\omega)| < 1/|w_I(j\omega)|$ as shown in (4) and (5).

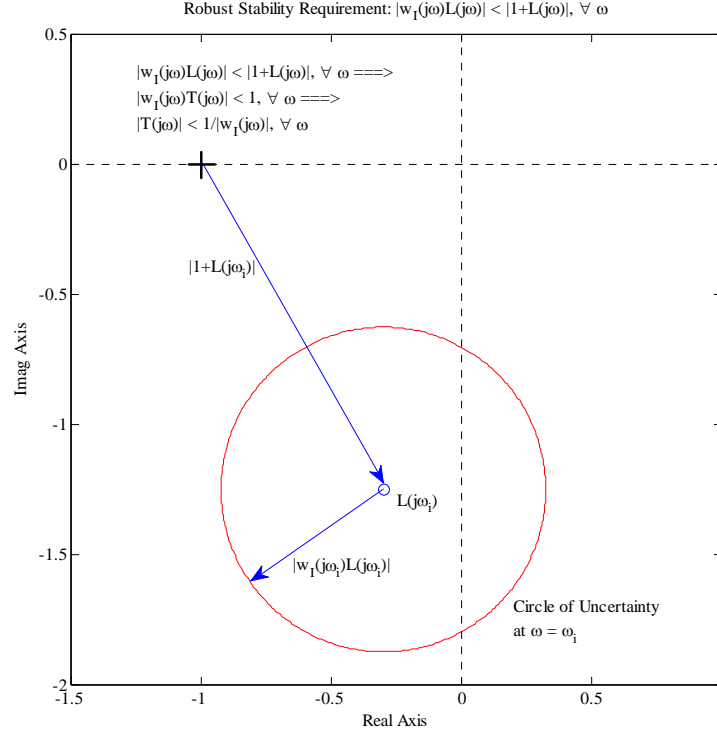


Fig. 4. Illustration of the robust stability requirement: $|T(j\omega)| < 1/|w_I(j\omega)|, \forall \omega$.

C. The Example

1) The Nominal and Extreme Plant Models:

A nominal plant and its Proportional + Integral (PI) controller are given by

$$G(s) = \frac{3(-2s+1)}{(5s+1)(10s+1)}, \quad K(s) = K_c \frac{(12.7s+1)}{12.7s} = K_c \frac{(s+0.07874)}{s} \quad (6)$$

The plant is non-minimum-phase, having a zero at $s = 0.5$. The initial value for the compensator gain is chosen to be $K_c = 1.13$, which was obtained by applying the Ziegler-Nichols method for determining the gains for PI controllers. This controller provides closed-loop stability for the nominal plant.

A specific “extreme” plant model is given by

$$G'(s) = \frac{4(-3s+1)}{(4s+1)} \quad (7)$$

This plant is an extreme model in this example in that it is as “far away as possible” from the nominal model $G(s)$ in a particular direction. Some value of $w_I \Delta_I$, with $|\Delta_I| = \rho = 1$, will generate this model from $G(s)$.

2) Uncertainty Weighting Function:

In order to determine the weighting function $w_I(s)$, the maximum magnitude of the relative uncertainty in the models must be determined. If a stable, low-order, rational function accurately describes this relative uncertainty, that function can be used as $w_I(s)$. In cases where the relative uncertainty magnitude cannot be modeled this way, then the actual function can be approximated by an overbounding stable, low-order transfer function. This approximating transfer function will be used as $w_I(s)$. The maximum magnitude of the relative uncertainty is given by

$$\begin{aligned} |l_I(j\omega)| &= \max_{G_P} \left| \frac{G_P(j\omega) - G(j\omega)}{G(j\omega)} \right| = \left| \frac{G'(j\omega) - G(j\omega)}{G(j\omega)} \right| \\ l_I(s) &= \frac{5.25s^3 - 0.2083s^2 - 0.3125s - 0.0104}{s^3 - 0.1875s - 0.0313} \end{aligned} \quad (8)$$

which has one pole and one zero in the right-half plane. The zero-frequency value for this function is 1/3, and the high-frequency value is 5.25. The magnitude of this function is 1 at approximately 0.1 r/s. A minimum-phase stable transfer function having

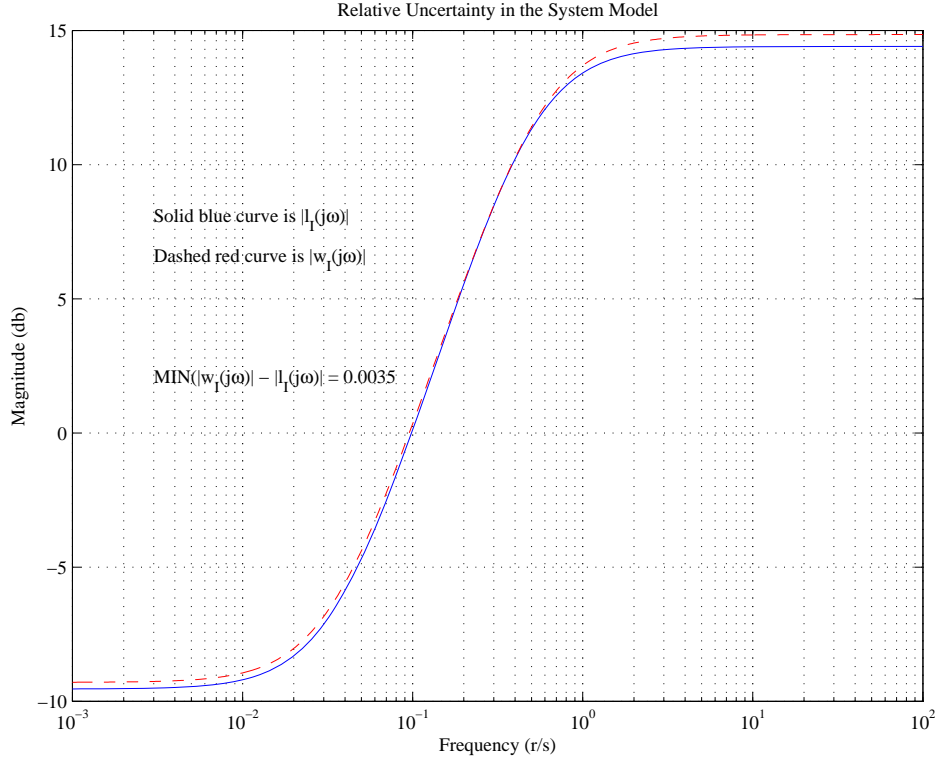


Fig. 5. Bode magnitude plots of the uncertainty function $l_I(s)$ and its overbounding function $w_I(s)$.

the same magnitude as $l_I(j\omega)$ at each frequency can be created by reflecting the right-half plane pole and zero into the left-half of the s -plane. As an alternative, a stable, first-order function that overbounds and reasonably approximates $l_I(s)$ could be used instead, one of which is given by

$$w_I(s) = \frac{10s + 0.343}{(10/5.525)s + 1} \quad (9)$$

The Bode magnitude plots for $l_I(j\omega)$ and $w_I(j\omega)$ in Fig. 5 demonstrate that the first-order, stable transfer function in (9) provides a complete—though somewhat conservative—overbounding of the actual uncertainty function $l_I(j\omega)$. It is certainly possible to find a different transfer function that provides a tighter overbounding, but that transfer function might require additional zeros and/or poles. With the transfer function given in (9), $|w_I(j\omega)| \geq |l_I(j\omega)| + 0.0035$, so complete overbounding of the actual uncertainty function is achieved. The magnitude of the transfer function for $w_I(s)$ in the text almost—but not completely—overbounds $|l_I(j\omega)|$. For the purposes of this example, the magnitude of the uncertainty function $w_I(j\omega)$ in (2) will be set equal to the magnitude of the actual uncertainty function $l_I(j\omega)$ since the magnitude of that function is the maximum relative magnitude of the perturbations. The remainder of this example will have $|w_I(j\omega)| = |l_I(j\omega)|$. The phase of the uncertainty function is not needed in the analysis of robust stability.

In order for a closed-loop system to be stable, the Nyquist stability criterion states that the polar plot of the open-loop transfer function must encircle the point $-1 + j0$ in the complex plane in the counter-clockwise direction one time for each unstable open-loop pole. Since the open-loop systems in this example have no right-half plane poles, that means that there must be no net encirclements of the -1 point. As previously mentioned, in order for the entire family of plant models to be stable (the robust stability requirement), the polar plot for each plant-compensator combination must avoid encircling the -1 point. The constraints given in (3)–(5) are repeated here.

$$\mathbf{RS:} \quad |w_I(j\omega) L(j\omega)| < |1 + L(j\omega)|, \quad \forall \omega \Rightarrow |w_I(j\omega) T(j\omega)| < 1, \quad \forall \omega \Rightarrow |T(j\omega)| < \frac{1}{|w_I(j\omega)|}, \quad \forall \omega \quad (10)$$

These conditions—which are equivalent—are both necessary and sufficient if the norm-bounded function Δ_I in (1) takes on all possible complex values (satisfying the norm bound) in generating the family of plant models. If the actual family of models is only a subset of the largest possible set, then the conditions are only sufficient, not necessary. In this case, the conditions on robust stability are conservative. You are protecting against loss of stability for some systems that cannot occur.

Bode plots of $|T(j\omega)|$ for two values of the compensator gain are shown in Fig. 6. When the initial value of gain is used, it is seen that the requirement $|T(j\omega)| < 1/|w_I(j\omega)|$ is not satisfied. This is the curve labeled T1 in the graph. If the compensator

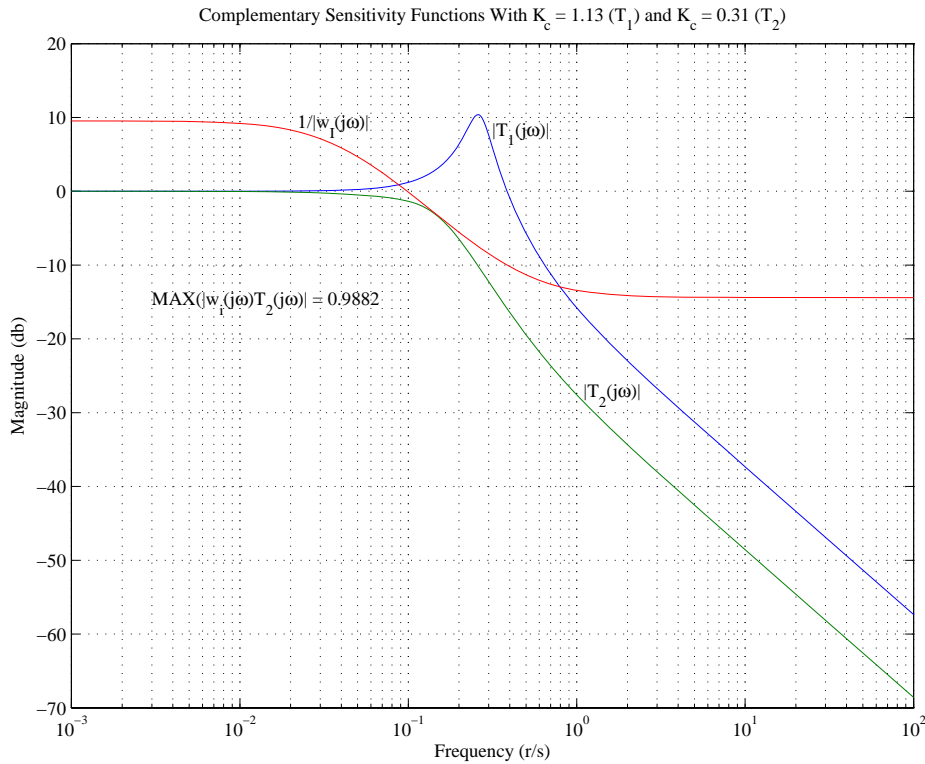


Fig. 6. Bode magnitude plots of inverse of the uncertainty function and the complementary sensitivity with two compensator gains.

gain is reduced to $K_c = 0.31$, then the magnitude of the complementary sensitivity is below the reciprocal of the magnitude of the weighting function at all frequencies. This is the curve labeled T2, with $|w_I(j\omega) T_2(j\omega)|_{\max} = 0.9882$. With this value of gain, all plant models in the family will be stabilized by $K(s)$.

The polar plots of the nominal and perturbed plants with the two compensator gains, shown in Fig. 7, illustrate the fact that the nominal model is stable with either gain, but the perturbed model is unstable with the initial gain. In each of the graphs, for those frequencies where the polar plot is inside the dashed circle centered at -1 , the magnitude of the sensitivity function, $|S(j\omega)| = 1/|1 + L(j\omega)|$, is greater than 1, which means that there will not be good reference tracking or disturbance rejection at those frequencies.

3) Evaluating the Stability Robustness:

The condition for robust stability given by the constraint on $|T(j\omega)|$ relative to $|w_I(j\omega)|$ can be shown graphically by superimposing circles of radius $|w_I(j\omega)L(j\omega)|$ on the polar plot of $L(j\omega)$. The condition for robust stability becomes the condition that no part of any of these circles representing the plant uncertainty can encircle the -1 point. If any one of the circles does encircle the -1 point, then there are some possible plant models that will not be stabilized. If any one of these plant models actually belongs to the family of plants, then the family obviously is not robustly stable. For the initial compensator gain $K_c = 1.13$, the circles in Fig. 8 are clearly seen to encircle the -1 point, so the family is not robustly stable with that gain, as was known from Fig. 6. For the second compensator gain $K_c = 0.31$, the circles in Fig. 9 are all inside the -1 point, so the family is robustly stable. However, if all possible plant models represented by the circle of uncertainty are in the family of systems to be controlled, then there will be some of those models on the verge of instability with the lower gain since the circles lie just inside the -1 point. The dashed curve in the figure is the perturbed plant model $G'(j\omega)$. Although it is an extreme model in the family of plants, it is not in the direction that takes it too close to the -1 point.

Although the polar plot for the extreme system $L'(s) = G'(s)K(s)$ looks “close” to the nominal systems’s polar plot and not close to the edges of the circles of uncertainty, it must be remembered that frequency is not shown on these plots. When points on the two polar plots are compared at the same frequency, it can be seen that the point on the extreme plot is the maximum distance away from the corresponding point on the nominal plot. This is illustrated in Fig. 10 at the frequency $\omega_i = 0.069$ r/s, where the two polar plots are shown along with the circle of uncertainty at that frequency. The small blue and red circles on the polar plots indicate the specific magnitudes and phases for $L(j\omega_i)$ and $L'(j\omega_i)$, respectively. The nominal system is the center of the circle of uncertainty, and the extreme system is on the circle, a distance $|w_I(j\omega_i)L(j\omega_i)|$ from the center.

For this particular extreme system, the perturbation is not in the worst-case direction—toward the -1 point—even though

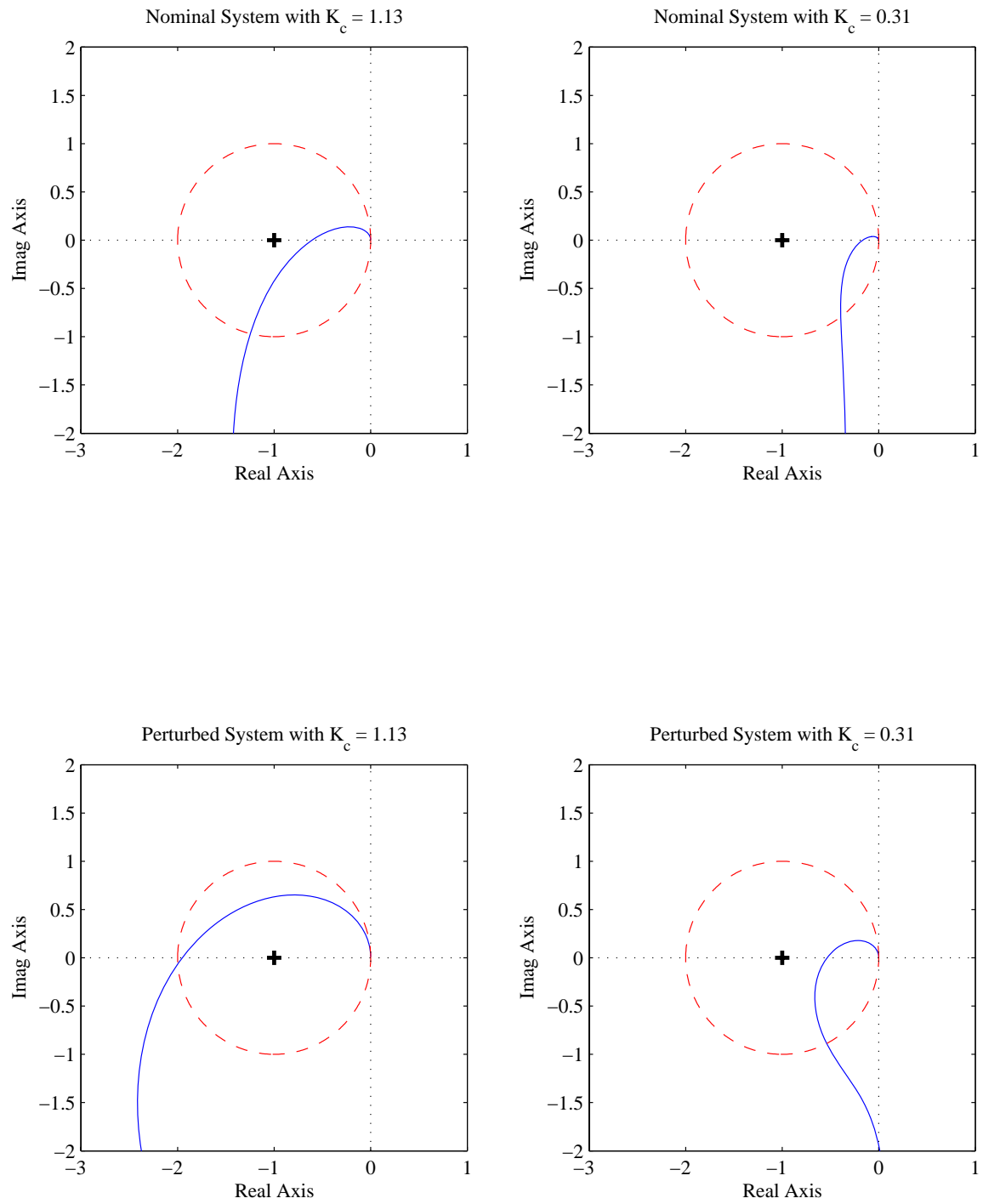


Fig. 7. Polar plots of the nominal and extreme systems with the two values of compensator gain.

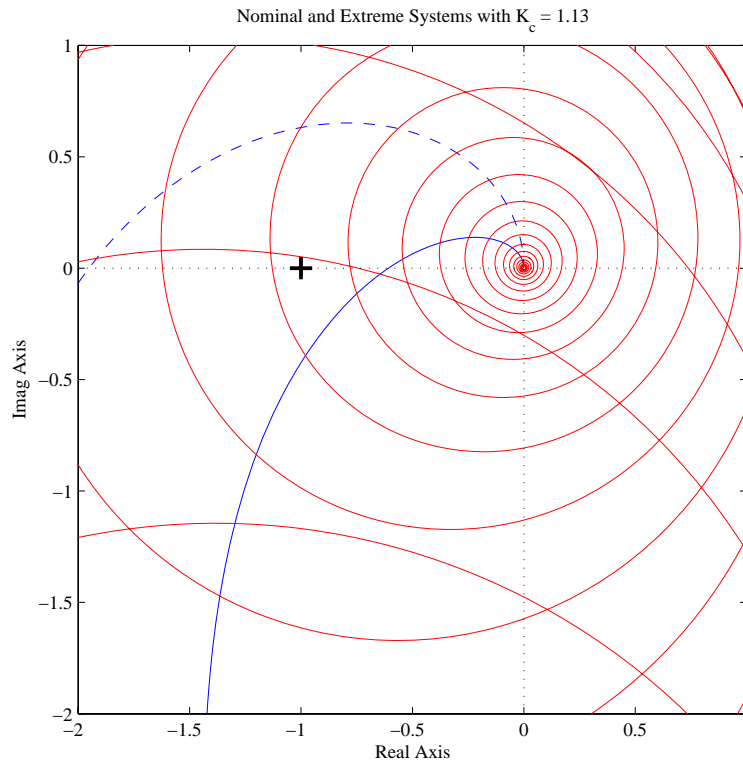


Fig. 8. Polar plots for the nominal and extreme systems with $K_c = 1.13$ and the circles of uncertainty illustrating the lack of robust stability.

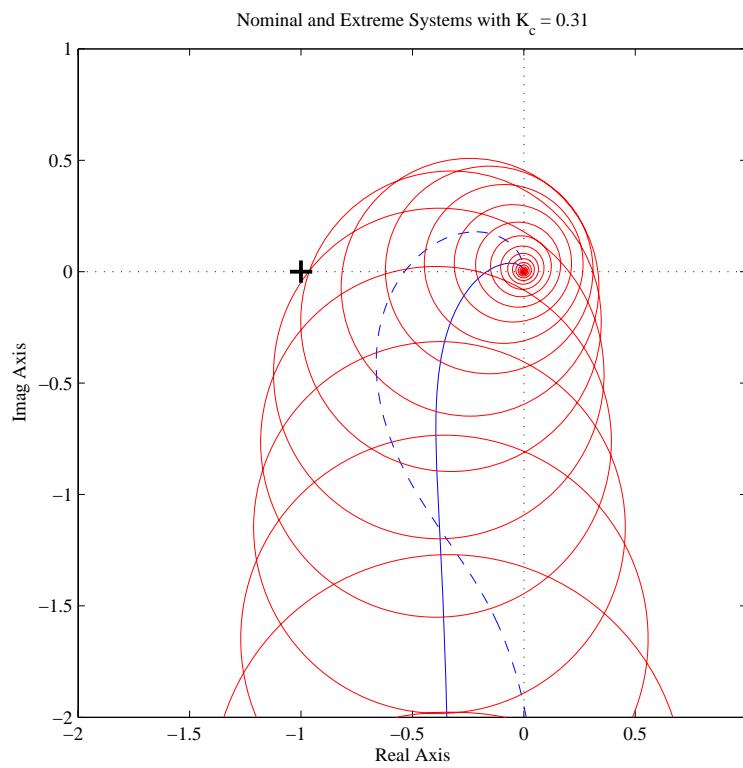


Fig. 9. Polar plots for the nominal and extreme systems with $K_c = 0.31$ and the circles of uncertainty illustrating robust stability.

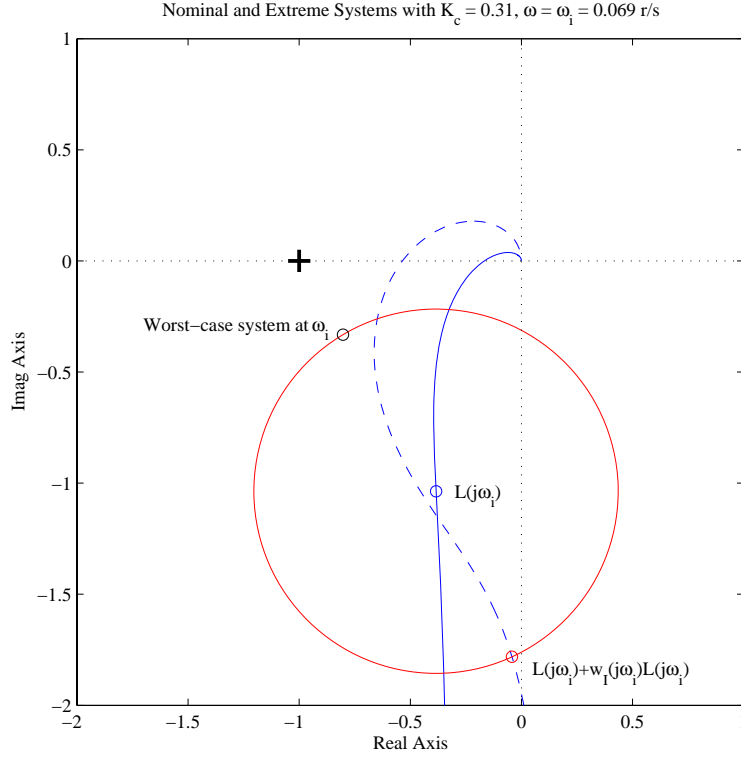


Fig. 10. Polar plots for the nominal and extreme systems with $K_c = 0.31$ and the circle of uncertainty at $\omega = 0.069$ r/s.

the magnitude of the perturbation is maximum at each frequency. The small black circle in Fig. 10 labeled “worst-case system” is at the point on the circle of uncertainty that is closest to the -1 point. The transfer function that would have the magnitude and phase at ω_i corresponding to that point is the worst-case system from the standpoint of being the system that is closest to instability. If the location of the point for an extreme system is known, the phase shift of $\Delta(j\omega)$ that would produce the corresponding perturbation to the nominal system can be computed from (2).

$$\angle \Delta(j\omega_i) = \angle [L'(j\omega_i) - L(j\omega_i)] - \angle w_I(j\omega_i) - \angle L(j\omega_i) \quad (11)$$

For the worst-case system in Fig. 10, $\angle \Delta(j\omega_i) = -173.9^\circ$ and $|\Delta(j\omega_i)| = 1$.

The polar plot for the system that has the worst-case magnitude and phase at each frequency is shown by the black line and circles in the top plot of Fig. 11. At each frequency, that system has the magnitude and phase which produces a point on the corresponding circle of uncertainty that is closer to the -1 point than any other point on the circle. It is the least stable system in the family. The frequency response for that system can be generated from that of the nominal system through some allowable perturbation $w_I(j\omega) L(j\omega) \Delta_I(j\omega)$, with $|\Delta_I(j\omega)| = 1$ and $\angle \Delta_I(j\omega) = \theta_{wc}(j\omega)$, where $\theta_{wc}(j\omega)$ is the phase shift needed to create the worst-case perturbation. The Bode magnitude and phase curves for the worst-case system are shown in the bottom plot of Fig. 11. It is interesting to note that the final value of the phase shift of the worst-case system is approximately -190° (this was verified up to $\omega = 10^5$ r/s). Since this is not an integer multiple of -90° , that system cannot be represented in standard transfer function form.

4) Classical Analysis of the Systems:

Classical ways of analyzing system stability and performance include the open-loop Bode plots and plots of the closed-loop step responses. The Bode plots in Fig. 12 show that both the nominal and perturbed systems have good phase margins with the reduced compensator gain. The nominal system is stable with the initial gain, but the phase margin is smaller than generally acceptable. The perturbed model with the initial gain is unstable, as indicated by the negative phase margin. Since the transfer functions of $L(s)$ and $L'(s)$ have one pole at the origin and a total of three poles and two zeros, the low-frequency and high-frequency slopes of the magnitude curves are -20 db/decade. However, since the systems have one zero in the right-half plane, which has the phase shift of a pole, from a phase shift standpoint, the systems have four poles and one zero. Therefore, the phase curves begin at -90° and end at -270° .

The step response plots in Fig. 13 show the qualitative connections between the phase margins and gain crossover frequencies in the frequency domain and the amounts of overshoot and the settling times in the time domain. Settling time in this example

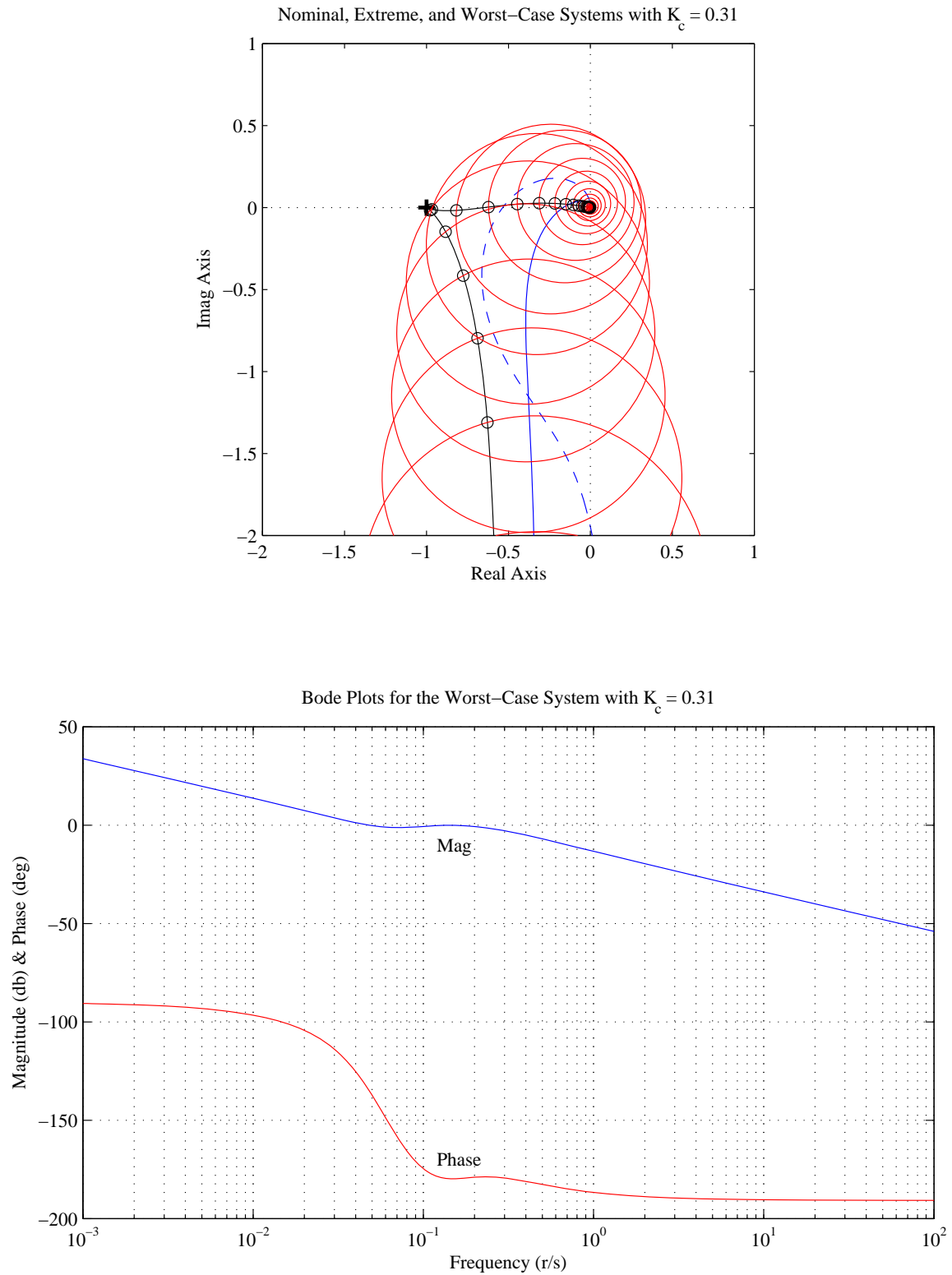


Fig. 11. Polar and Bode plots for the worst-case system, with $K_c = 0.31$.

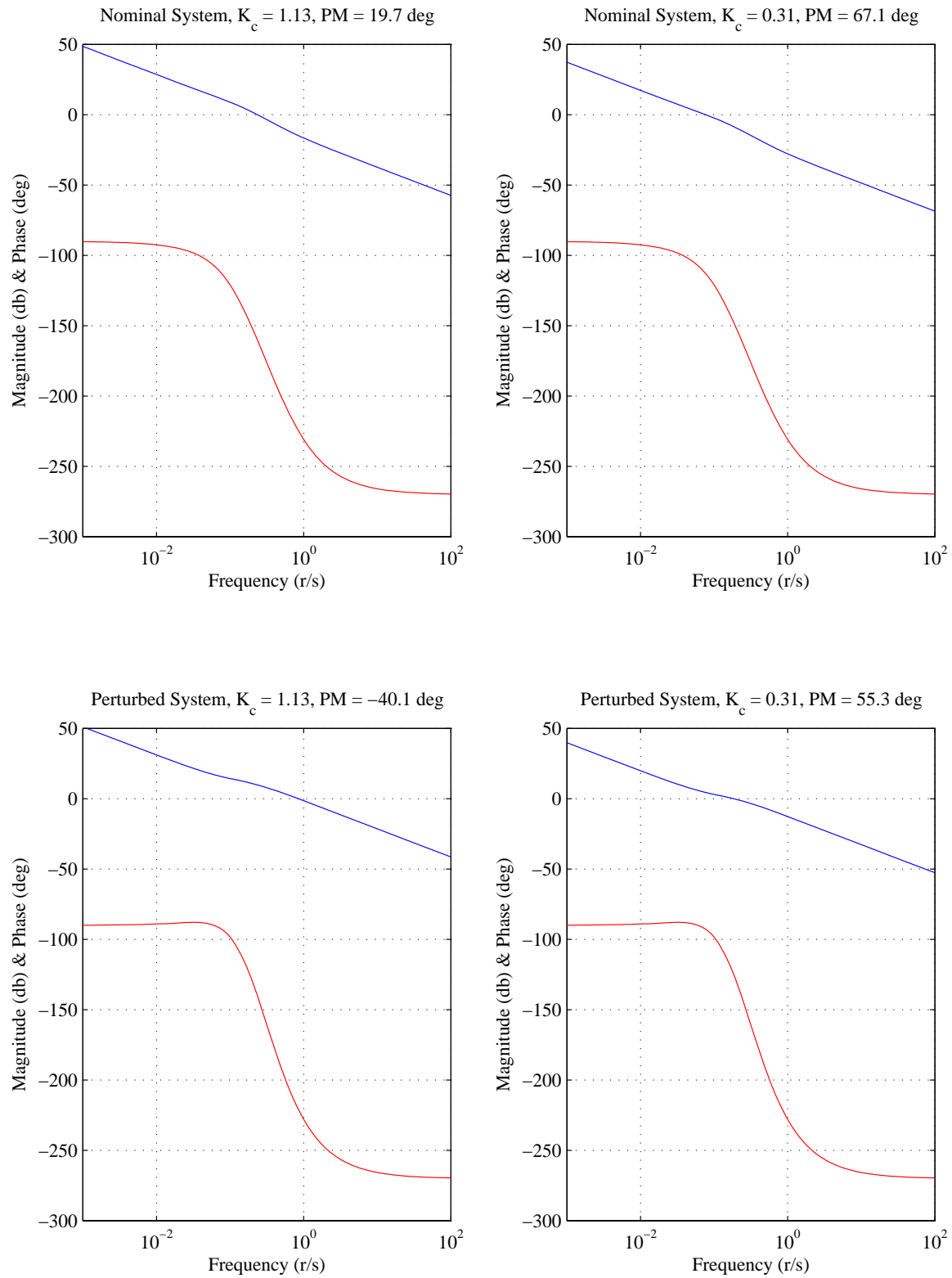


Fig. 12. Bode plots for the nominal and extreme systems with compensator gains $K_c = 1.13$ and $K_c = 0.31$.

is defined as the time it takes the step response to get within and stay within $\pm 2\%$ of the final value. Since the systems each have one pole at the origin, the final values of the step responses are equal to the value of the reference input.

The combination of nominal plant and initial compensator yields a stable response, but one that exhibits a large overshoot, oscillations, and a long settling time. This would generally be considered an unacceptable response. Both of the systems with the reduced compensator gain have much smaller overshoot, fewer oscillations, and much shorter settling times. Although the perturbed system's response has more overshoot and a longer settling time than the nominal system, it has clearly has a stable response, which might be considered acceptable. The instability of the perturbed model with the initial compensator gain is evident.

It can be noted in each of the stable step responses that the output signal initially goes negative instead of positive. This is known as an inverse response, which is due to the non-minimum-phase zero in each of the plant models. Further discussion of non-minimum-phase zeros and the inverse response can be found at http://teal.gmu.edu/~gbeale/ece_720/examples_720.html.

D. Concluding Comments

This example has presented the development of the condition for robust stability imposed on the complementary sensitivity function $T(s)$ when the uncertainty in the plant model is represented as a multiplicative perturbation. The condition has been illustrated through an example from the text by Skogestad and Postlethwaite. Failing to satisfy this condition was shown to prevent some of the system models from being stabilized. Satisfying the condition guarantees that each of the plant models in the family will be closed-loop stable. The use of the Nyquist stability criterion was used to derive the condition for robust stability.

It should be noted that providing robust stability for a family of systems does not guarantee that the time-domain performance of each of the systems in the family will be acceptable, only that it will be stable. In order to ensure good performance for the members of the family of systems, the concept of robust performance must be employed. Notes on robust performance design can be found on the same website mentioned above.

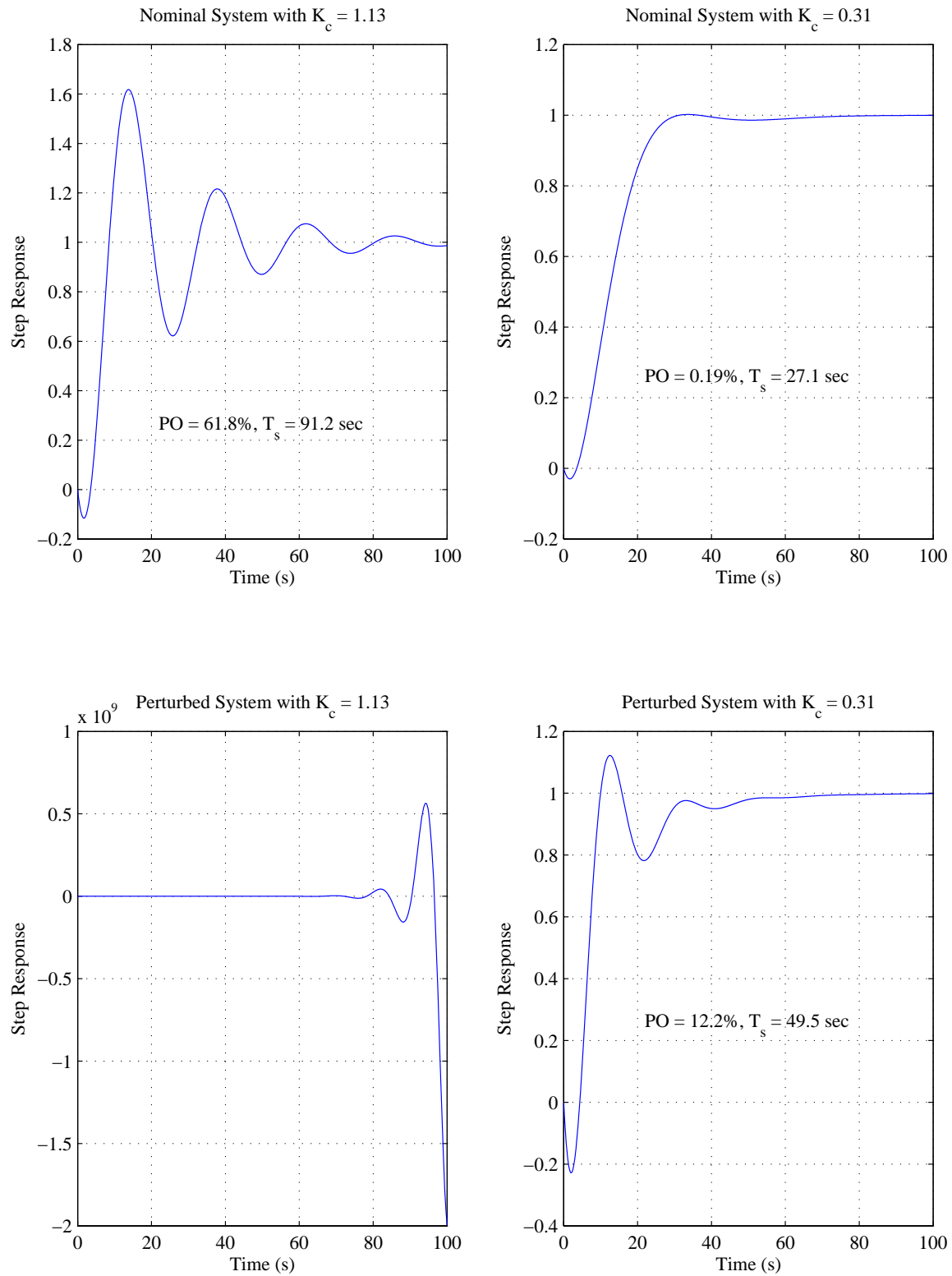


Fig. 13. Closed-loop step responses for the nominal and extreme systems with compensator gains $K_c = 1.13$ and $K_c = 0.31$.